

Data-driven spatio-temporal discretization for pedestrian flow characterization

Marija Nikolić, Michel Bierlaire

August 23, 2017

Outline

Introduction

Methodology

Application

Conclusion

Urbanization

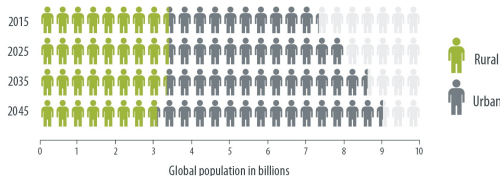
1950: **30%** of the population lives in cities

2014: **54%** of the population lives in cities

Challenges

Energy consumption, pollution, climate change

Increased traffic and congestion



Source: UN World Urbanization Prospects: 2011 Revision

Congestion: Pedestrian movements



Research challenges

Understand, describe and predict

Optimization of current
infrastructure and operations

Efficient planning and management
of future pedestrian facilities

Characterization

Quantities

Density k (ped/m²)

Speed v (m/s)

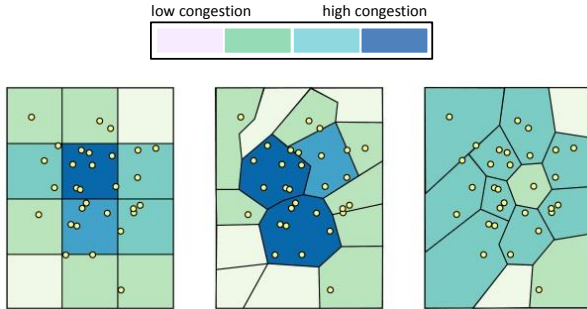
Flow q (ped/m·s)

Limitations

Highly inspired by vehicular traffic

Arbitrary spatial and temporal discretization

Discretization



Research challenges

Results sensitive to minor changes

Arbitrary discretization may introduce noise in data

How to define the discretization...

...independent of arbitrary chosen values?



How to define the discretization...

...independent of arbitrary chosen values?



Data-driven approach: Voronoi diagrams

Outline

Introduction

Methodology

Application

Conclusion

Context

Model

Space-time representation: $\Omega \subset \mathbb{R}^3$

Units: meters and seconds

$p = (x, y, t) \in \Omega$: physical position (x, y) in space at a specific time t

Assumption: Ω is convex (obstacle-free and bounded)

Data: trajectories

Continuous: $\Gamma_i : \{p_i(t) | p_i(t) = (x_i(t), y_i(t), t)\}$

Discrete (sample):

$\Gamma_i : \{p_{is} | p_{is} = (x_{is}, y_{is}, t_s)\}, t_s = [t_0, t_1, \dots, t_f]$

3D Voronoi diagrams: 3DVoro

Definition

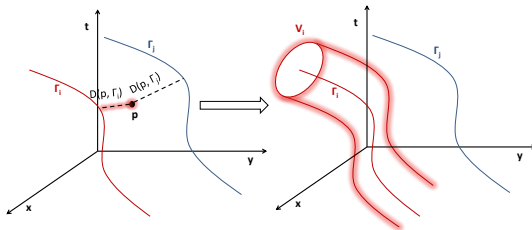
Associate $p \in \Omega$ with the closest Γ_i :

Voronoi cell for Γ_i :

$$\delta_{\Gamma}(p, \Gamma_i) = \begin{cases} 1, & D(p, \Gamma_i) \leq D(p, \Gamma_j), \forall j \\ 0, & \text{otherwise} \end{cases}$$

$$V_i = \{p \in | \delta_{\Gamma}(p, \Gamma_i) = 1 \}$$

$$D(p, \Gamma_i) = \min_{p_i} \{d(p, p_i)\}$$



3DVoro: Distances

Spatial Euclidean distance

$$d_E(p, p_i) = \begin{cases} \sqrt{(x - x_i)^2 + (y - y_i)^2}, & t = t_i; \\ \infty, & \text{otherwise} \end{cases}$$

Each point in time is independent

Motivated by the availability of snapshots of the floor area

All pedestrians must be observed at the exact same time

3DVoro: Distances

Time-Transform distances

$$d_{TT_1}(p, p_i) = \sqrt{(x - x_i)^2 + (y - y_i)^2 + v^2(t - t_i)^2}$$

$$d_{TT_2}(p, p_i) = \sqrt{(x - x_i)^2 + (y - y_i)^2 + \hat{v}_i(t_i)^2(t - t_i)^2}$$

$$d_{TT_3}(p, p_i) = \sqrt{(x - x_i)^2 + (y - y_i)^2} + \hat{v}_i(t_i)|t - t_i|$$

Convert seconds into meters using speed

$d_{TT_1}(p, p_i)$, $d_{TT_2}(p, p_i)$: combine components based on the Euclidean norm

d_{TT_3} : weighted sum of two norms

3DVoro: Distances

Predictive distance

$$d_P(p, p_i) = \begin{cases} \sqrt{(x_i^a - x)^2 + (y_i^a - y)^2}, & t - t_i \geq 0 \\ \infty, & \text{otherwise} \end{cases}$$

$$x_i^a = x_i^a(t) = x_i + (t - t_i)v_i^x(t_i)$$

$$y_i^a = y_i^a(t) = y_i + (t - t_i)v_i^y(t_i)$$

Accounts for the pedestrian dynamics

Anticipates future position when performing the assignment

Anticipation time: from zero to $t - t_i$

Points backward in time: infinitely distant

3DVoro: Distances

Mahalanobis distance

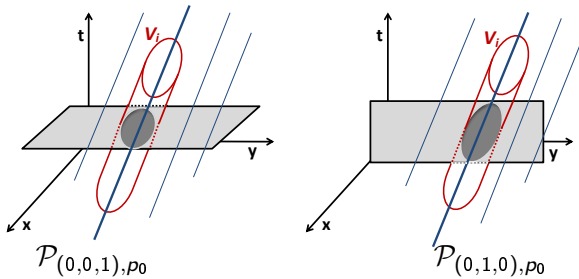
$$d_M(p, p_i) = \sqrt{(p - p_i)^T M_i (p - p_i)}$$

M_i : a change of variable matrix

Points in the movement direction of a pedestrian are “closer” than the points from other directions

Intersection with a plane

$\mathcal{P}_{(a,b,c),p_0}$: plane through p_0 with normal vector (a, b, c)



Voronoi-based traffic quantities

Consider $(x, y, t) \in \Omega$, and i such that $(x, y, t) \in V_i$

Density: $k(x, y, t) = \frac{1}{|V_i \cap \mathcal{P}_{(0,0,1),(x,y,t)}|}$

Flow: $\vec{q}_{(a,b,0)}(x, y, t) = \frac{1}{|V_i \cap \mathcal{P}_{(a,b,0),(x,y,t)}|}$

Velocity: $\vec{v}_{(a,b,0)}(x, y, t) = \frac{|V_i \cap \mathcal{P}_{(0,0,1),(x,y,t)}|}{|V_i \cap \mathcal{P}_{(a,b,0),(x,y,t)}|}$

Outline

Introduction

Methodology

Application

Conclusion

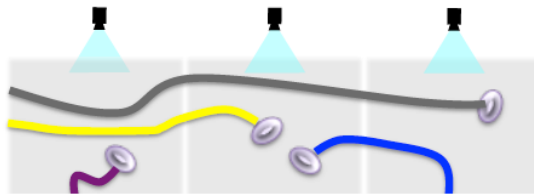
Lausanne train station



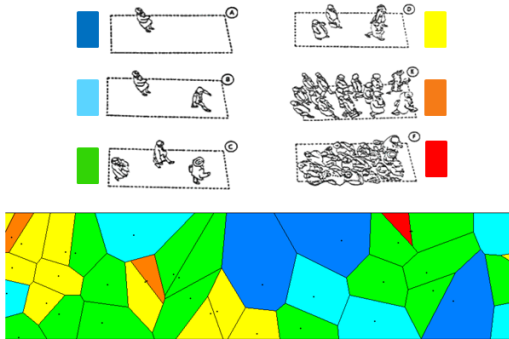
Lausanne train station: Data set

A large-scale network of smart sensors: a sparsity driven tracking (Alahi et al., 2014)

Dataset: 25,603 trajectories; February 2013

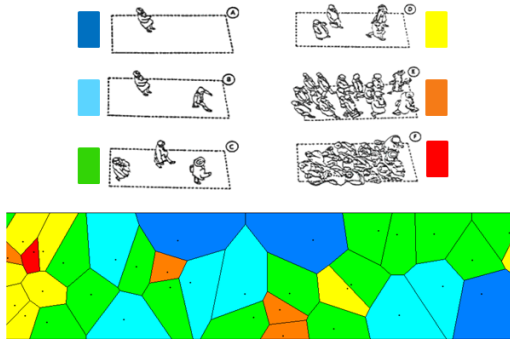


3DVoro illustration: Lausanne train station



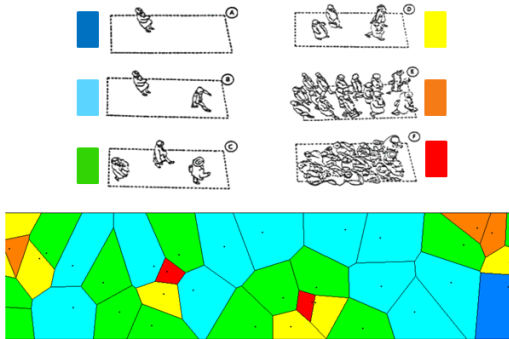
- Data-driven discretization
- General framework
- Microscopic characterization
- Applicable to continuous and discrete data

3DVoro illustration: Lausanne train station



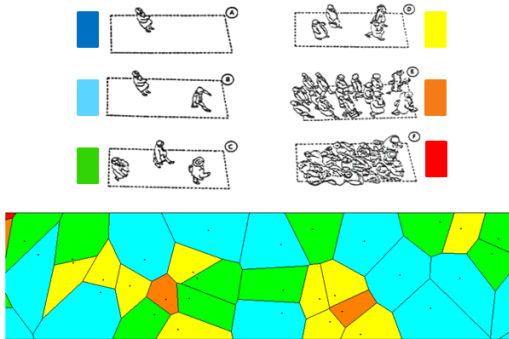
- Data-driven discretization
- General framework
- Microscopic characterization
- Applicable to continuous and discrete data

3DVoro illustration: Lausanne train station



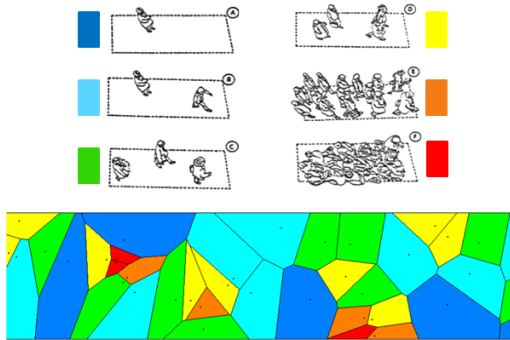
- Data-driven discretization
- General framework
- Microscopic characterization
- Applicable to continuous and discrete data

3DVoro illustration: Lausanne train station



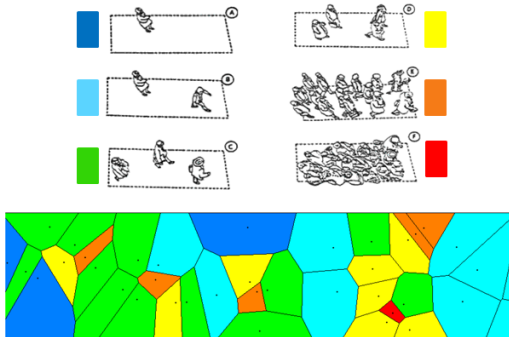
- Data-driven discretization
- General framework
- Microscopic characterization
- Applicable to continuous and discrete data

3DVoro illustration: Lausanne train station



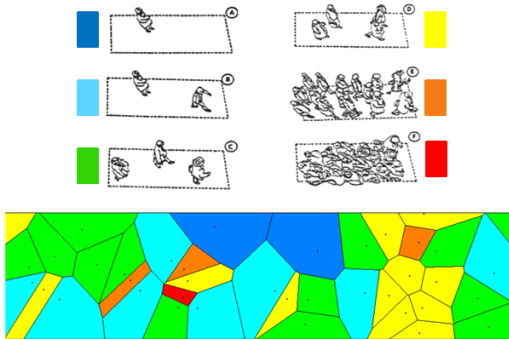
- Data-driven discretization
- General framework
- Microscopic characterization
- Applicable to continuous and discrete data

3DVoro illustration: Lausanne train station



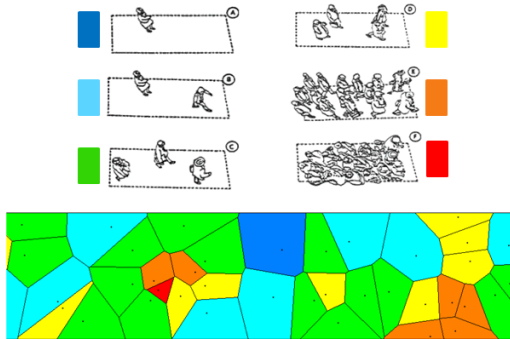
- Data-driven discretization
- General framework
- Microscopic characterization
- Applicable to continuous and discrete data

3DVoro illustration: Lausanne train station



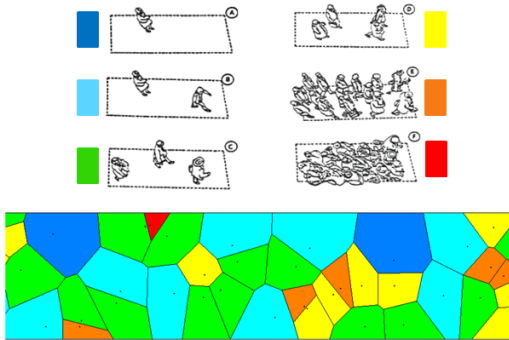
- Data-driven discretization
- General framework
- Microscopic characterization
- Applicable to continuous and discrete data

3DVoro illustration: Lausanne train station



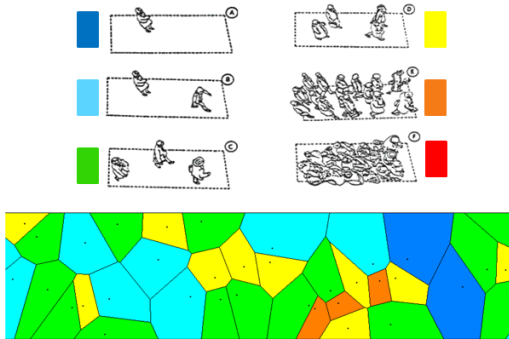
- Data-driven discretization
- General framework
- Microscopic characterization
- Applicable to continuous and discrete data

3DVoro illustration: Lausanne train station



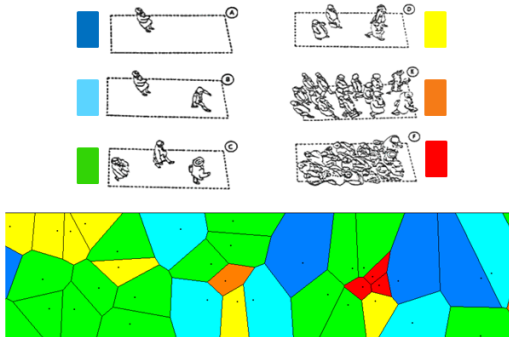
- Data-driven discretization
- General framework
- Microscopic characterization
- Applicable to continuous and discrete data

3DVoro illustration: Lausanne train station



- Data-driven discretization
- General framework
- Microscopic characterization
- Applicable to continuous and discrete data

3DVoro illustration: Lausanne train station



- Data-driven discretization
- General framework
- Microscopic characterization
- Applicable to continuous and discrete data

3DVoro performance: Synthetic data

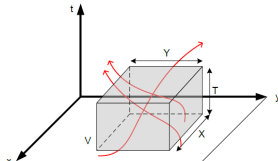
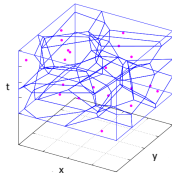
NOMAD simulation tool (Campanella et al.; 2014)

Flow composition: uni-directional and bi-directional

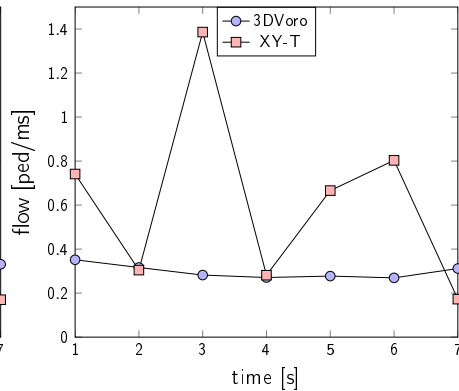
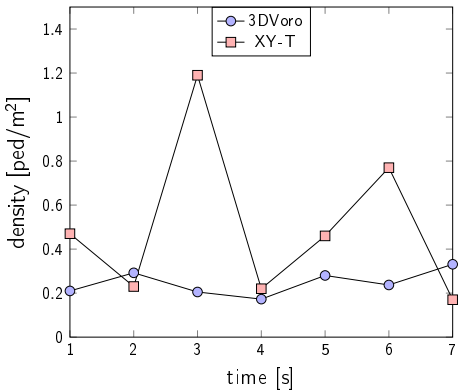
Scenarios: low/high demand, homogenous/heterogeneous population

Analysis

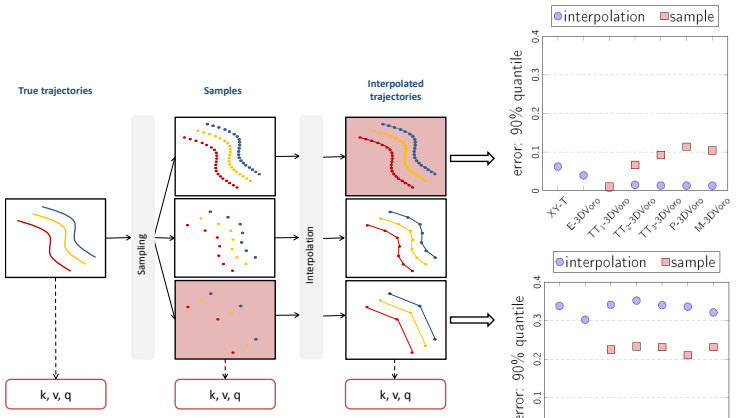
3DVoro and XY-T methods



Nature of the results



Robustness to sampling of trajectories



Outline

Introduction

Methodology

Application

Conclusion

Conclusion

Main findings

Data-driven spatio-temporal discretization

Well defined, flexible and general framework

Smooth transitions in measured characteristics

Robust to noise in the data

Robust to sampling of trajectories

Future directions

Anisotropy and presence of obstacles

Thank you

Intelligent Traffic Control and Service in Big Data Environment
Data-driven spatio-temporal discretization for pedestrian flow characterization

Marija Nikolić, Michel Bierlaire

- marija.nikolic@epfl.ch



References |

- Campanella, M., Hoogendoorn, S. and Daamen, W. (2014). The nomad model: theory, developments and applications, *Transportation Research Procedia* 2: 462–467.
- Edie, L. C. (1963). *Discussion of traffic stream measurements and definitions*, Port of New York Authority, New York, USA.
- Fruin, J. J. (1971). Designing for pedestrians: A level-of-service concept, number 355, Highway Research Board, Washington, DC, pp. 1–15.

References ||

- Helbing, D., Johansson, A. and Al-Abideen, H. Z. (2007). Dynamics of crowd disasters: An empirical study, *Physical review E - Statistical, Nonlinear, and Soft Matter Physics* **75**(4): 1–7.
- Jabari, S. E., Zheng, J. and Liu, H. X. (2014). A probabilistic stationary speed–density relation based on Newell's simplified car-following model, *Transportation Research Part B: Methodological* **68**: 205–223.
- Saberi, M. and Mahmassani, H. (2014). Exploring areawide dynamics of pedestrian crowds: Three-dimensional approach, *Transportation Research Record: Journal of the Transportation Research Board* **2421**(1): 31–40.

References III

Steffen, B. and Seyfried, A. (2010). Methods for measuring pedestrian density, flow, speed and direction with minimal scatter, *Physica A: Statistical mechanics and its applications* 389(9): 1902–1910.

van Wageningen-Kessels, F., Hoogendoorn, S. P. and Daamen, W. (2014). Extension of Edie's definitions for pedestrian dynamics, *Transportation Research Procedia* 2: 507–512.

Characteristics of methods

Method	Scale	Spatial aggregation		Temporal aggregation		Data type
		Unit	Assumptions	Unit	Assumptions	
XY-T	Macroscopic	Area	Shape Size Location	Interval	Duration	Trajectories
Grid-based (GB)	Macroscopic	Cell	Size Location	Interval	Duration	Trajectories Sync. sample
Range-based (RB)	Macroscopic	Circle	Radius Location	Interval	Duration	Trajectories Sync. sample
Exponentially-weighted (EW)	Macroscopic	Range	Influence function Range of influence	Interval	Duration	Trajectories Sync. sample
Voronoi-based (VB)	Microscopic	Voronoi cell	Boundary conditions	Interval	Duration	Trajectories Sync. sample

3DVoro: Distances

Mahalanobis distance

$$S_1(t_i, \alpha) = p_i + \Delta t v_i(t_i) + \alpha d^1(t_i)$$

$$d^1(t_i) = \frac{v_i(t_i)}{\|v_i(t_i)\|}, \|d^1(t_i)\| = 1$$

$$S_2(t_i, \alpha) = p_i - \Delta t v_i(t_i) - \alpha d^1(t_i)$$

$$S_3(t_i, \alpha) = p_i + \alpha d^2(t_i)$$

$$d^2(t_i) = \begin{pmatrix} d_x^1(t_i) \\ d_y^2(t_i) \\ 0 \end{pmatrix}$$

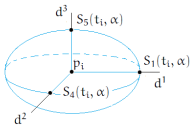
$$S_4(t_i, \alpha) = p_i - \alpha d^2(t_i)$$

$$d^3(t_i) = \begin{pmatrix} 0 \\ 0 \\ \Delta t \end{pmatrix}$$

$$S_5(t_i, \alpha) = p_i + \alpha d^3(t_i)$$

$$S_6(t_i, \alpha) = p_i - \alpha d^3(t_i)$$

$$d_M(S_j, p_i) = \alpha, j = 1, \dots, 6$$

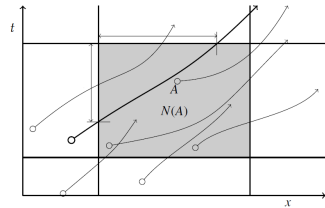


Edie (1963)

$$k(A) = \frac{\sum_{i=1}^N t_i}{dxdt}$$

$$q(A) = \frac{\sum_{i=1}^N x_i}{dxdt}$$

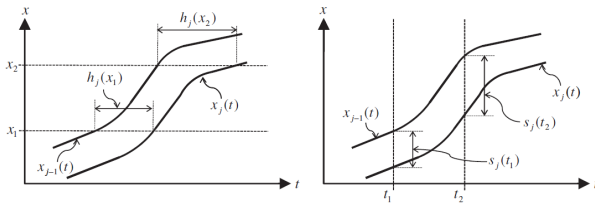
$$v(A) = \frac{\sum_{i=1}^N x_i}{\sum_{i=1}^N t_i}$$



$$k(x, t) = \frac{1}{s_i(t)}, \text{ for } x \in [x_i(t), x_{i-1}(t)]$$

$$q(x, t) = \frac{1}{h_i(x)}, \text{ for } t \in (t_{i-1}(x), t_i(x)]$$

$$v(x, t) = \frac{s_i(t)}{h_i(x)}, \text{ for } x \in [x_i(t), x_{i-1}(t)], t \in (t_{i-1}(x), t_i(x)]$$

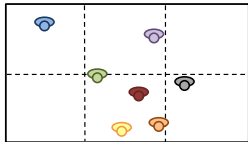


Fruin (1971)

$$k(x, y, t) = \frac{N_A(t)}{|A|}, \text{ for } (x, y) \in A$$

$$\vec{q}(x, y, t) = k(x, y, t) \vec{v}(x, y, t)$$

$$\vec{v}_i(t) = \frac{\begin{pmatrix} x_i(t_2) \\ y_i(t_2) \end{pmatrix} - \begin{pmatrix} x_i(t_1) \\ y_i(t_1) \end{pmatrix}}{t_2 - t_1}$$



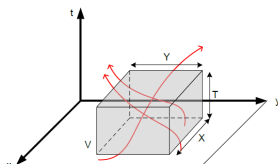
$$\vec{v}(x, y, t) = \frac{\sum_{i=1}^{N_A} \vec{v}_i(t)}{N_A}, \text{ for } (x, y) \in A$$

van Wageningen-Kessels et al. (2014)
Saberi and Mahmassani (2014)

$$k(A) = \frac{\sum_{i=1}^N t_i}{dxdydt}$$

$$\vec{q}(A) = \begin{pmatrix} q_x(A) \\ q_y(A) \end{pmatrix} = \begin{pmatrix} \sum_{i=1}^N x_i \\ \frac{dxdydt}{\sum_{i=1}^N y_i} \\ \sum_{i=1}^N y_i \\ \frac{dxdydt}{\sum_{i=1}^N y_i} \end{pmatrix}$$

$$\vec{v}(A) = \begin{pmatrix} v_x(A) \\ v_y(A) \end{pmatrix} = \begin{pmatrix} \sum_{i=1}^N x_i \\ \frac{\sum_{i=1}^N t_i}{\sum_{i=1}^N y_i} \\ \sum_{i=1}^N y_i \\ \frac{\sum_{i=1}^N t_i}{\sum_{i=1}^N y_i} \end{pmatrix}$$

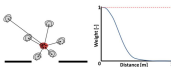


Helbing et al. (2007)

$$f\left(\begin{pmatrix} x_i(t) \\ y_i(t) \end{pmatrix} - \begin{pmatrix} x \\ y \end{pmatrix}\right) = \frac{1}{\pi R^2} \exp\left(-\frac{\left\|\begin{pmatrix} x_i(t) \\ y_i(t) \end{pmatrix} - \begin{pmatrix} x \\ y \end{pmatrix}\right\|^2}{R^2}\right)$$

$$k(x, y, t) = \sum_i f\left(\begin{pmatrix} x_i(t) \\ y_i(t) \end{pmatrix} - \begin{pmatrix} x \\ y \end{pmatrix}\right)$$

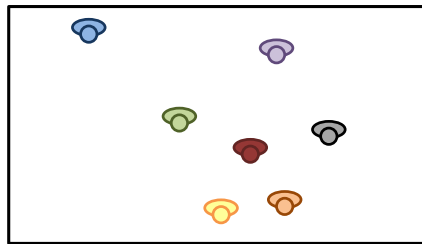
$$\bar{q}(x, y, t) = k(x, y, t) \vec{v}(x, y, t)$$



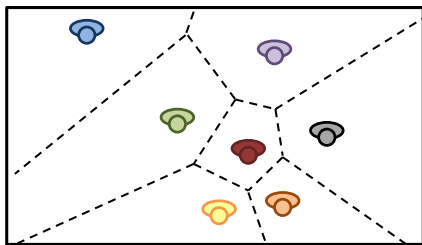
$$\vec{v}_i(t) = \frac{\begin{pmatrix} x_i(t_2) \\ y_i(t_2) \end{pmatrix} - \begin{pmatrix} x_i(t_1) \\ y_i(t_1) \end{pmatrix}}{t_2 - t_1}$$

$$\vec{v}(x, y, t) = \frac{\sum_i \vec{v}_i(t) f\left(\begin{pmatrix} x_i(t) \\ y_i(t) \end{pmatrix} - \begin{pmatrix} x \\ y \end{pmatrix}\right)}{\sum_i f\left(\begin{pmatrix} x_i(t) \\ y_i(t) \end{pmatrix} - \begin{pmatrix} x \\ y \end{pmatrix}\right)}$$

Voronoi diagrams: 2D

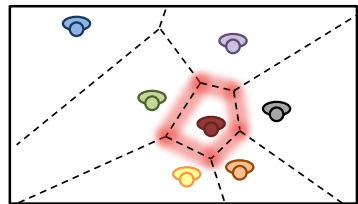


Voronoi diagrams: 2D



$$k(x, y, t) = \frac{1}{|A_i|}, \text{ for } (x, y) \in A_i$$

$$\vec{v}(x, y, t) = \frac{\begin{pmatrix} x_i(t_2) \\ y_i(t_2) \end{pmatrix} - \begin{pmatrix} x_i(t_1) \\ y_i(t_1) \end{pmatrix}}{t_2 - t_1}$$



q : half a person has passed a segment if half of the Voronoi cell has passed it

Lausanne data

Tracklet generation

A graph-based tracking algorithm is implemented to link the detected points

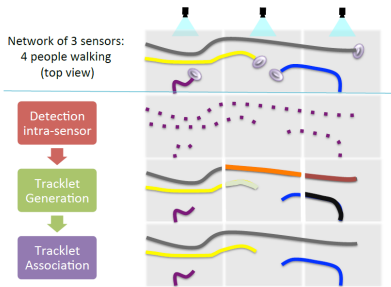
A directed graph: vertices representing the 3D coordinates of detected pedestrians, edges defining the connectivity between vertices

The connectivity prevents too long or unrealistic connections

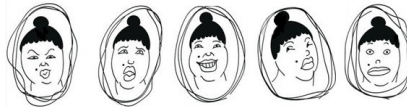
Tracklet association

Task: find the set of trajectories Θ that best explains the extracted tracklets

Formally: maximizing the a-posterior probability of Θ given the set of tracklets



3DVoro: Robustness to noise in the data



100 sets of pedestrian trajectories synthesized per scenario

$\theta_r^M(p) = (k_r^M(p), v_r^M(p), q_r^M(p))$: a vector of indicators at point p obtained by applying the method M to the r^{th} set of trajectories

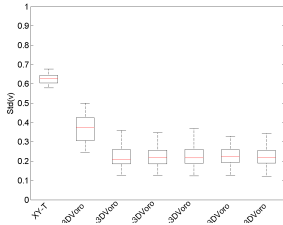
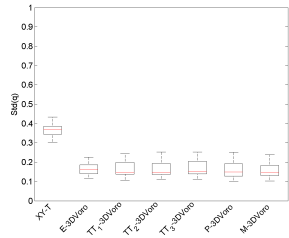
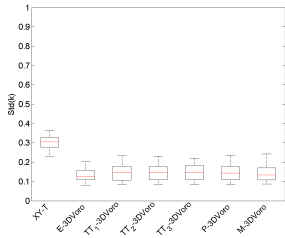
The standard deviation of the indicators at p as

$$\sigma_R^M(p) = \sqrt{\frac{1}{R} \sum_{r=1}^R (\theta_r^M(p) - \mu_R^M(p))^2}$$

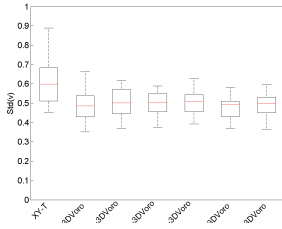
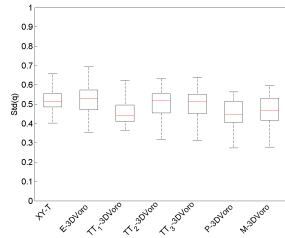
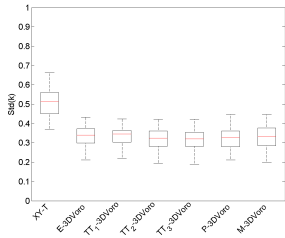
$$\mu_R^M(p) = \frac{1}{R} \sum_{r=1}^R \theta_r^M(p), R = 100$$

The procedure is repeated for 1000 randomly selected points p

3DVoro: Robustness to noise in the data - Sc.I



3DVoro: Robustness to noise in the data - Sc.II



3DVoro: Robustness to sampling frequency

Method	Mean		Mode		Median		90% quantile	
	IT	SoP	IT	SoP	IT	SoP	IT	SoP
XY-T	$1.47e^{-02}$	/	$1.25e^{-02}$	/	$1.25e^{-02}$	/	$6.25e^{-02}$	/
E-3DVoro	$1.17e^{-02}$	/	0	/	$4.48e^{-04}$	/	$3.96e^{-02}$	/
TT ₁ -3DVoro	$2.70e^{-03}$	$6.70e^{-03}$	0	0	$3.00e^{-04}$	$2.30e^{-03}$	$7.30e^{-03}$	$1.02e^{-02}$
TT ₂ -3DVoro	$5.80e^{-03}$	$3.50e^{-02}$	0	$2.80e^{-03}$	$6.00e^{-04}$	$2.08e^{-02}$	$1.50e^{-02}$	$6.69e^{-02}$
TT ₃ -3DVoro	$5.40e^{-03}$	$4.34e^{-02}$	0	$8.00e^{-03}$	$6.00e^{-04}$	$2.83e^{-02}$	$1.32e^{-02}$	$9.22e^{-02}$
P-3DVoro	$8.20e^{-03}$	$5.36e^{-02}$	0	$6.10e^{-03}$	$2.40e^{-03}$	$3.03e^{-02}$	$1.30e^{-02}$	$1.14e^{-01}$
M-3DVoro	$4.50e^{-03}$	$5.65e^{-02}$	0	$6.80e^{-03}$	$1.10e^{-03}$	$4.55e^{-02}$	$1.28e^{-02}$	$1.04e^{-01}$

(a) Sampling frequency: $3 s^{-1}$

Method	Mean		Mode		Median		90% quantile	
	IT	SoP	IT	SoP	IT	SoP	IT	SoP
XY-T	$1.90e^{-01}$	/	$1.00e^{-01}$	/	$1.50e^{-01}$	/	$3.38e^{-01}$	/
E-3DVoro	$1.64e^{-01}$	/	$1.12e^{-02}$	/	$1.46e^{-01}$	/	$3.02e^{-01}$	/
TT ₁ -3DVoro	$2.54e^{-01}$	$1.27e^{-01}$	$1.35e^{-02}$	$9.00e^{-03}$	$1.16e^{-01}$	$8.97e^{-02}$	$3.41e^{-01}$	$2.25e^{-01}$
TT ₂ -3DVoro	$1.64e^{-01}$	$1.22e^{-01}$	$1.44e^{-02}$	$1.06e^{-02}$	$1.21e^{-01}$	$7.30e^{-02}$	$3.52e^{-01}$	$2.33e^{-01}$
TT ₃ -3DVoro	$1.89e^{-01}$	$1.24e^{-01}$	$1.84e^{-02}$	$1.09e^{-02}$	$1.24e^{-01}$	$7.88e^{-02}$	$3.40e^{-01}$	$2.31e^{-01}$
P-3DVoro	$3.19e^{-01}$	$1.21e^{-01}$	$3.26e^{-02}$	$6.20e^{-03}$	$1.43e^{-01}$	$7.43e^{-02}$	$3.36e^{-01}$	$2.10e^{-01}$
M-3DVoro	$1.97e^{-01}$	$1.24e^{-01}$	$3.48e^{-02}$	$9.90e^{-03}$	$1.41e^{-01}$	$7.72e^{-02}$	$3.21e^{-01}$	$2.31e^{-01}$

(b) Sampling frequency: $0.5 s^{-1}$

Robustness to the sampling frequency of density indicator - $Uni_{LD-HomoPop}$

3DVoro: Robustness to sampling frequency

Method	Mean		Mode		Median		90% quantile	
	IT	SoP	IT	SoP	IT	SoP	IT	SoP
XY-T	2.05e-02	/	0	/	1.25e-02	/	5.00e-02	/
E-3DVoro	1.43e-02	/	0	/	2.67e-02	/	2.64e-02	/
TT1-3DVoro	8.00e-03	4.55e-02	0	0	8.00e-04	1.75e-02	2.36e-02	8.52e-02
TT2-3DVoro	1.49e-02	1.07e-01	0	0	3.20e-03	5.72e-02	3.33e-02	2.21e-01
TT3-3DVoro	1.24e-02	1.60e-01	0	0	3.50e-03	9.62e-02	2.98e-02	3.41e-01
P-3DVoro	2.10e-02	1.66e-01	0	0	4.20e-03	1.16e-01	5.27e-02	3.64e-01
M-3DVoro	1.31e-02	2.40e-01	0	0	2.50e-03	1.75e-01	2.91e-02	5.58e-01

(a) Sampling frequency: 3 s^{-1}

Method	Mean		Mode		Median		90% quantile	
	IT	SoP	IT	SoP	IT	SoP	IT	SoP
XY-T	5.29e-01	/	1.63e-01	/	4.75e-01	/	1.01e+00	/
E-3DVoro	4.02e-01	/	0	/	2.49e-01	/	1.03E+00	/
TT1-3DVoro	4.06e-01	2.90e-01	3.10e-01	2.48e-02	2.64e-01	1.65e-01	9.21e-01	7.12e-01
TT2-3DVoro	3.92e-01	4.58e-01	2.85e-01	2.34e-01	2.48e-01	2.34e-01	9.30e-01	1.11E+00
TT3-3DVoro	4.41e-01	5.07e-01	2.89e-01	5.89e-02	2.37e-01	3.06e-01	9.81e-01	1.17E+00
P-3DVoro	4.31e-01	3.71e-01	1.40e-03	0	2.58e-01	1.80e-01	9.43e-01	7.29e-01
M-3DVoro	4.34e-01	5.01e-01	3.16e-01	1.36e-01	2.75e-01	3.52e-01	9.96e-01	9.80e-01

(b) Sampling frequency: 0.5 s^{-1}

Robustness to the sampling frequency of density indicator - *UniHD-HeteroPop*

3DVoro: Robustness to sampling frequency

Method	Mean		Mode		Median		90% quantile	
	IT	SoP	IT	SoP	IT	SoP	IT	SoP
XY-T	6.50e-02	/	0	/	0	/	8.65e-03	/
E-3DVoro	1.20e-02	/	0	/	0	/	4.66e-03	/
TT ₁ -3DVoro	3.58e-03	1.08e-02	0	0	0	1.02e-03	4.16e-03	6.15e-03
TT ₂ -3DVoro	8.13e-03	1.18e-02	0	0	0	2.35e-03	8.09e-03	1.29e-02
TT ₃ -3DVoro	1.49e-02	2.06e-02	0	3.91e-03	0	8.43e-03	7.46e-03	3.10e-02
P-3DVoro	2.29e-02	5.42e-02	0	1.94e-03	0	2.72e-02	9.25e-03	1.06e-01
M-3DVoro	2.15e-02	4.82e-02	0	4.31e-02	0	2.42e-02	7.69e-03	1.29e-01

(a) Sampling frequency: 3 s^{-1}

Method	Mean		Mode		Median		90% quantile	
	IT	SoP	IT	SoP	IT	SoP	IT	SoP
XY-T	1.66e-01	/	0	/	6.84e-02	/	7.00e-01	/
E-3DVoro	1.65e-01	/	0	/	1.19e-01	/	3.40e-01	/
TT ₁ -3DVoro	1.68e-01	1.29e-01	3.50e-02	5.02e-02	8.50e-02	5.70e-02	3.85e-01	2.62e-01
TT ₂ -3DVoro	1.70e-01	1.02e-01	4.52e-02	5.63e-02	8.49e-02	6.15e-02	3.82e-01	5.57e-01
TT ₃ -3DVoro	1.80e-01	1.18e-01	4.82e-02	6.06e-02	8.80e-02	6.55e-02	3.83e-01	2.65e-01
P-3DVoro	2.02e-01	1.60e-01	3.69e-02	4.84e-02	9.36e-02	6.73e-02	4.14e-01	3.01e-01
M-3DVoro	1.80e-01	1.55e-01	4.80e-02	3.36e-02	1.01e-01	9.27e-02	4.38e-01	3.08e-01

(b) Sampling frequency: 0.5 s^{-1}

Robustness to the sampling frequency of density indicator - $Bi_{LD-HomoPop}$

3DVoro: Robustness to sampling frequency

Method	Mean		Mode		Median		90% quantile	
	IT	SoP	IT	SoP	IT	SoP	IT	SoP
XY-T	$2.85e^{-02}$	/	0	/	$3.28e^{-03}$	/	$1.00e^{-01}$	/
E-3DVoro	$3.00e^{-02}$	/	0	/	$9.64e^{-03}$	/	$6.50e^{-02}$	/
TT ₁ -3DVoro	$1.15e^{-01}$	$2.78e^{-02}$	0	0	$7.90e^{-04}$	$8.78e^{-03}$	$2.32e^{-02}$	$4.94e^{-02}$
TT ₂ -3DVoro	$9.72e^{-02}$	$9.34e^{-02}$	0	0	$3.21e^{-03}$	$5.16e^{-02}$	$3.50e^{-02}$	$2.15e^{-01}$
TT ₃ -3DVoro	$4.89e^{-02}$	$1.05e^{-01}$	0	0	$2.83e^{-03}$	$5.91e^{-02}$	$3.56e^{-02}$	$2.62e^{-01}$
P-3DVoro	$1.15e^{-01}$	$1.70e^{-01}$	0	$3.33e^{-02}$	$4.79e^{-03}$	$6.28e^{-02}$	$4.65e^{-02}$	$2.61e^{-01}$
M-3DVoro	$1.15e^{-01}$	$1.52e^{-01}$	0	$8.33e^{-02}$	$4.55e^{-03}$	$7.20e^{-02}$	$5.35e^{-02}$	$3.51e^{-01}$

(a) Sampling frequency: 3 s^{-1}

Method	Mean		Mode		Median		90% quantile	
	IT	SoP	IT	SoP	IT	SoP	IT	SoP
XY-T								
E-3DVoro	$2.79e^{-01}$	/	0	/	$1.29e^{-01}$	/	$7.14e^{-01}$	/
TT ₁ -3DVoro	$4.49e^{-01}$	$2.58e^{-01}$	$5.70e^{-03}$	$1.99e^{-03}$	$1.54e^{-01}$	$1.34e^{-01}$	$8.43e^{-01}$	$6.64e^{-01}$
TT ₂ -3DVoro	$3.71e^{-01}$	$2.98e^{-01}$	$4.28e^{-02}$	$9.34e^{-02}$	$1.61e^{-01}$	$1.40e^{-01}$	$8.07e^{-01}$	$7.90e^{-01}$
TT ₃ -3DVoro	$9.82e^{-01}$	$3.56e^{-01}$	$4.34e^{-02}$	$6.70e^{-03}$	$1.64e^{-01}$	$1.38e^{-01}$	$7.76e^{-01}$	$7.74e^{-01}$
P-3DVoro	$3.82e^{-01}$	$3.15e^{-01}$	$2.32e^{-03}$	$6.74e^{-03}$	$1.53e^{-01}$	$1.61e^{-01}$	$9.09e^{-01}$	$7.22e^{-01}$
M-3DVoro	$4.08e^{-01}$	$3.77e^{-01}$	$1.89e^{-02}$	$1.47e^{-02}$	$1.90e^{-01}$	$1.74e^{-01}$	$7.91e^{-01}$	$8.18e^{-01}$

(b) Sampling frequency: 0.5 s^{-1}

Robustness to the sampling frequency of density indicator - $Bi_{HD-HeteroPop}$

3DVoro: Robustness to sampling frequency

Method	Mean		Mode		Median		90% quantile	
	IT	SoP	IT	SoP	IT	SoP	IT	SoP
XY-T	4.30e ⁻⁰³	/	0	/	3.40e ⁻⁰³	/	1.16e ⁻⁰²	/
E-3DVoro	1.55e ⁻⁰¹	/	0	/	3.56e ⁻⁰²	/	4.99e ⁻⁰¹	/
TT ₁ -3DVoro	9.60e ⁻⁰³	2.31e ⁻⁰²	0	0	2.20e ⁻⁰³	9.38e ⁻⁰³	2.79e ⁻⁰²	4.85e ⁻⁰²
TT ₂ -3DVoro	2.04e ⁻⁰²	7.66e ⁻⁰²	0	4.10e ⁻⁰³	5.80e ⁻⁰³	4.48e ⁻⁰²	6.48e ⁻⁰²	1.68e ⁻⁰¹
TT ₃ -3DVoro	1.81e ⁻⁰²	9.15e ⁻⁰²	0	8.00e ⁻⁰⁴	5.70e ⁻⁰³	4.51e ⁻⁰²	5.42e ⁻⁰²	2.15e ⁻⁰¹
P-3DVoro	2.98e ⁻⁰²	1.38e ⁻⁰¹	0	5.90e ⁻⁰³	1.41e ⁻⁰²	7.90e ⁻⁰²	5.75e ⁻⁰²	2.92e ⁻⁰¹
M-3DVoro	1.88e ⁻⁰²	1.46e ⁻⁰¹	0	2.00e ⁻⁰⁴	5.90e ⁻⁰³	1.04e ⁻⁰¹	5.95e ⁻⁰²	3.22e ⁻⁰¹

(a) Sampling frequency: 3 s^{-1}

Method	Mean		Mode		Median		90% quantile	
	IT	SoP	IT	SoP	IT	SoP	IT	SoP
XY-T	5.80e ⁻⁰¹	/	1.02	/	3.26e ⁻⁰¹	/	1.42	/
E-3DVoro	1.77	/	4.36e ⁻⁰²	/	7.11e ⁻⁰¹	/	1.27	/
TT ₁ -3DVoro	5.42e ⁻⁰¹	5.40e ⁻⁰¹	2.28e ⁻⁰²	2.10e ⁻⁰³	3.43e ⁻⁰¹	3.02e ⁻⁰¹	1.04	9.66e ⁻⁰¹
TT ₂ -3DVoro	5.11e ⁻⁰¹	5.56e ⁻⁰¹	1.39e ⁻⁰¹	8.20e ⁻⁰³	3.15e ⁻⁰¹	3.17e ⁻⁰¹	1.07	1.04
TT ₃ -3DVoro	6.08e ⁻⁰¹	5.52e ⁻⁰¹	3.72e ⁻⁰²	7.50e ⁻⁰³	3.29e ⁻⁰¹	3.18e ⁻⁰¹	1.05	1.05
P-3DVoro	5.60e ⁻⁰¹	5.41e ⁻⁰¹	8.75e ⁻⁰²	1.30e ⁻⁰³	3.32e ⁻⁰¹	3.04e ⁻⁰¹	9.76e ⁻⁰¹	9.82e ⁻⁰¹
M-3DVoro	5.03e ⁻⁰¹	5.43e ⁻⁰¹	3.93e ⁻⁰²	6.91e ⁻⁰²	3.76e ⁻⁰¹	3.15e ⁻⁰¹	1.08	9.52e ⁻⁰¹

(b) Sampling frequency: 0.5 s^{-1}

Robustness to the sampling frequency of velocity indicator - $Uni_{LD-HomoPop}$

3DVoro: Robustness to sampling frequency

Method	Mean		Mode		Median		90% quantile	
	IT	SoP	IT	SoP	IT	SoP	IT	SoP
XY-T	$1.92e^{-02}$	/	$9.60e^{-03}$	/	$6.20e^{-03}$	/	$3.42e^{-02}$	/
E-3DVoro	$3.17e^{-02}$	/	0	/	$6.30e^{-03}$	/	$3.86e^{-02}$	/
TT ₁ -3DVoro	$1.57e^{-02}$	$6.18e^{-02}$	0	0	$6.10e^{-03}$	$1.87e^{-02}$	$3.23e^{-02}$	$1.30e^{-01}$
TT ₂ -3DVoro	$1.83e^{-02}$	$1.38e^{-01}$	0	$1.73e^{-02}$	$7.90e^{-03}$	$4.27e^{-02}$	$3.82e^{-02}$	$3.88e^{-01}$
TT ₃ -3DVoro	$1.85e^{-02}$	$1.88e^{-01}$	0	$1.00e^{-01}$	$8.00e^{-03}$	$6.46e^{-02}$	$4.08e^{-02}$	$4.87e^{-01}$
P-3DVoro	$2.93e^{-02}$	$2.05e^{-01}$	0	$7.96e^{-02}$	$9.00e^{-03}$	$9.82e^{-02}$	$6.49e^{-02}$	$5.29e^{-01}$
M-3DVoro	$2.14e^{-02}$	$3.16e^{-01}$	0	$5.10e^{-03}$	$8.00e^{-03}$	$1.47e^{-01}$	$4.37e^{-02}$	$8.21e^{-01}$

(a) Sampling frequency: 3 s^{-1}

Method	Mean		Mode		Median		90% quantile	
	IT	SoP	IT	SoP	IT	SoP	IT	SoP
XY-T	$5.73e^{-01}$	/	1.15	/	$3.51e^{-01}$	/	1.58	/
E-3DVoro	1.01	/	$8.57e^{-01}$	/	$3.85e^{-01}$	/	1.67	/
TT ₁ -3DVoro	$5.82e^{-01}$	$5.80e^{-01}$	$8.69e^{-01}$	$5.85e^{-02}$	$4.51e^{-01}$	$3.13e^{-01}$	1.40	1.28
TT ₂ -3DVoro	$5.76e^{-01}$	$5.67e^{-01}$	$9.40e^{-01}$	$1.02e^{-01}$	$3.75e^{-01}$	$2.64e^{-01}$	1.54	1.16
TT ₃ -3DVoro	$5.79e^{-01}$	$5.94e^{-01}$	$8.50e^{-01}$	$5.73e^{-02}$	$3.70e^{-01}$	$2.77e^{-01}$	1.46	1.29
P-3DVoro	$5.66e^{-01}$	$5.62e^{-01}$	$8.92e^{-01}$	$4.61e^{-02}$	$3.83e^{-01}$	$2.95e^{-01}$	1.38	1.26
M-3DVoro	$6.27e^{-01}$	$7.11e^{-01}$	$9.13e^{-01}$	$1.43e^{-02}$	$5.05e^{-01}$	$2.86e^{-01}$	1.55	1.49

(b) Sampling frequency: 0.5 s^{-1}

Robustness to the sampling frequency of velocity indicator - *UniHD-HeteroPop*

3DVoro: Robustness to sampling frequency

Method	Mean		Mode		Median		90% quantile	
	IT	SoP	IT	SoP	IT	SoP	IT	SoP
XY-T	1.93e-02	/	0	/	1.77e-02	/	7.73e-02	/
E-3DVoro	1.65e-02	/	0	/	5.60e-03	/	3.75e-02	/
TT1-3DVoro	3.00e-04	7.60e-03	0	0	0	2.60e-03	8.00e-04	1.74e-02
TT2-3DVoro	1.40e-03	4.16e-02	0	0	0	3.17e-02	3.60e-03	8.99e-02
TT3-3DVoro	1.30e-03	4.65e-02	0	4.32e-02	0	3.48e-02	3.90e-03	1.14e-01
P-3DVoro	2.70e-03	4.69e-02	0	1.41e-02	8.00e-04	2.27e-02	5.50e-03	1.29e-01
M-3DVoro	1.20e-03	5.09e-02	0	4.75e-02	0	3.54e-02	2.50e-03	1.23e-01

(a) Sampling frequency: 3 s^{-1}

Method	Mean		Mode		Median		90% quantile	
	IT	SoP	IT	SoP	IT	SoP	IT	SoP
XY-T	2.55e-01	/	1.45e-01	/	2.45e-01	/	5.06e-01	/
E-3DVoro	4.17e-01	/	6.50e-02	/	1.27e-01	/	3.83e-01	/
3DVoro- δ_{TT_1}	1.74e-01	1.50e-01	1.79e-01	8.00e-04	1.13e-01	8.77e-02	3.21e-01	2.98e-01
TT1-3DVoro	2.07e-01	1.53e-01	1.92e-01	1.00e-04	1.39e-01	8.52e-02	3.71e-01	3.29e-01
TT2-3DVoro	2.33e-01	1.52e-01	2.05e-01	3.00e-04	1.48e-01	8.46e-02	3.63e-01	3.27e-01
TT2-3DVoro	2.17e-01	1.43e-01	1.53e-01	1.40e-03	1.34e-01	8.49e-02	3.01e-01	2.98e-01
M-3DVoro	1.75e-01	1.48e-01	1.83e-01	1.00e-04	1.36e-01	9.11e-02	3.43e-01	3.22e-01

(b) Sampling frequency: 0.5 s^{-1}

Robustness to the sampling frequency of flow indicator - $Uni_{LD-HomoPop}$

3DVoro: Robustness to sampling frequency

Method	Mean		Mode		Median		90% quantile	
	IT	SoP	IT	SoP	IT	SoP	IT	SoP
XY-T	2.75e-02	/	2.30e-03	/	1.75e-02	/	7.21e-02	/
E-3DVoro	1.09e-02	/	0	/	8.70e-04	/	2.83e-02	/
TT ₁ -3DVoro	7.80e-03	6.06e-02	0	0	7.00e-04	1.21e-02	2.22e-02	1.58e-01
TT ₂ -3DVoro	1.05e-02	1.45e-01	0	0	1.10e-03	6.08e-02	2.78e-02	3.11e-01
TT ₃ -3DVoro	1.06e-02	2.03e-01	0	0	1.00e-03	8.27e-02	2.19e-02	4.64e-01
P-3DVoro	1.62e-02	1.95e-01	0	4.86e-02	1.80e-03	8.54e-02	3.70e-02	4.90e-01
M-3DVoro	1.29e-02	3.06e-01	0	0	1.60e-03	1.48e-01	2.92e-02	8.95e-01

(a) Sampling frequency: 3 s^{-1}

Method	Mean		Mode		Median		90% quantile	
	IT	SoP	IT	SoP	IT	SoP	IT	SoP
XY-T	5.18e-01	/	3.50e-01	/	4.48e-01	/	1.09	/
E-3DVoro	6.54e-01	/	3.69e-01	/	2.03e-01	/	1.54	/
TT ₁ -3DVoro	4.99e-01	4.02e-01	1.06e-01	6.49e-02	3.24e-01	1.81e-01	1.35	9.43e-01
TT ₂ -3DVoro	5.66e-01	4.16e-01	1.47e-01	5.55e-02	2.73e-01	1.73e-01	1.57	1.21
TT ₃ -3DVoro	5.91e-01	4.45e-01	1.53e-01	1.57e-01	2.94e-01	1.71e-01	1.68	1.31
P-3DVoro	4.81e-01	4.28e-01	5.53e-02	3.98e-02	2.22e-01	1.89e-01	1.34	1.12
M-3DVoro	6.41e-01	4.47e-01	9.07e-02	4.55e-02	3.97e-01	1.73e-01	1.66	1.24

(b) Sampling frequency: 0.5 s^{-1}

Robustness to the sampling frequency of flow indicator - *UniHD-HeteroPop*

3DVoro: Robustness to sampling frequency

Interpolation

Higher sampling frequency

Time-Transform distances lead to the best performance (TT1-3DVoro)

Samples

Lower sampling frequency

$Uni_{LD-HomoPop}$: the distances that take into account the speed and/or direction of pedestrians (TT₂-3DVoro, P-3DVoro and M-3DVoro)

$Uni_{HD-HeteroPop}$: Time- Transform distances (TT₁-3DVoro)

General

Time-Transform: more data available (the sampling frequency equal to 3 s^{-1} or the demand equal to 3.6 pedestrians per second)

Distances accounting for the dynamics: less data available (the sampling frequency equal to 0.5 s^{-1} and the demand equal to 1.2 pedestrians per second)